A Tale of Two Complexes, [$PtMe_n$(RN=CH–CH=NR)] ($n = 2$ and $n = 4$, R = Cyclohexyl): Why do Pt^{II} and Pt^{IV} Complexes Exhibit Virtually Identical Redox Behavior and Colors?

Steffen Hasenzahl, Hans-Dieter Hausen, and Wolfgang Kaim*

Abstract: In spite of their very similar cyclic voltammograms, absorption spectra, and solvatochromic behavior, the two 1,4-diazabutadiene title complexes exhibit markedly different photoreactivities and underlying electronic structures, as evident from absorption and EPR spectra of the persistent anion radical forms. The lowest excited state of the nonphotoreactive Pt^{II} system [(CyN=CH–CH=NCy)-$PtMe_2$] has MLCT (metal-to-ligand charge-transfer, $5d \rightarrow \pi^*$) character, and the EPR spectrum of the corresponding anion radical at $\langle g \rangle = 2.016$ exhibits sizable metal/ligand orbital mixing. On the other hand, the structurally characterized Pt^{IV} complex [(CyN=CH–CH=NCy)-$PtMe_4$] ($C2/c$; $a = 2021.6(2)$, $b = 805.3(1)$, $c = 1254.2(1)$ pm; $\beta = 111.05(1)°$; $V = 1905.7(4) \times 10^6$ pm^3; $Z = 4$) has a low-lying photoreactive LLCT (ligand-to-ligand charge-transfer, $\sigma_{Pt-C} \rightarrow \pi^*$) excited state in which the axial Pt–C bonds are activated, as already suggested by the longer Pt–C(ax) bonds (214.0(8) pm) relative to Pt–C(eq) in the ground state (204.5(5) pm). The anion radical of the Pt^{IV} complex has lost the long-wavelength absorption band in the visible; it shows a well-resolved EPR spectrum at $\langle g \rangle = 1.9945$ with π-ligand and ^{195}Pt hyperfine structure and a small g anisotropy. A qualitative MO scheme is presented to account for the similar frontier-orbital energy differences despite dissimilar underlying electronic structures.

Keywords
charge transfer · EPR spectroscopy · organometallic compounds · platinum compounds · spectroelectrochemistry

Introduction

Complexes between the small, chelating and πelectron-accepting 1,4-diazabutadiene (DAB) ligands[1, 2] and electron-rich (organo)metallic complex fragments are generally distinguished by intense, solvatochromic[3] "charge-transfer" colors and by facile one-electron reduction to complexes containing the corresponding DAB radical anion.[2, 4] However, it has been noted in the past that the electrons available for charge transfer from the DAB-coordinating metal fragment can originate from filled d orbitals of d^6, d^8, or d^{10} centers[1, 2, 5, 6] (metal-to-ligand charge-transfer, MLCT), or from electron-rich metal–"carbanion" σ bonds of organometallics containing a metal in a "normal" oxidation state[4] (ligand-to-ligand charge-transfer, LLCT). In this contribution we report that the distinction between the two cases is not easy to make on the basis of conventional spectroscopic or electrochemical data alone, but that more detailed insight into the different electronic structures and the resulting different reactivity can be gained by absorption and, in particular, EPR spectra of singly reduced complexes. We have employed the 1,4-dialkylated DAB ligand CyN=CH–CH=NCy (Cy = cyclohexyl), with its small, four-center π chromophore, in connection with two rather simple organometallic fragments, $PtMe_n$ ($n = 2$ and 4), with different oxidation states (II and IV) and coordination numbers (4 and 6) of the metal (Fig. 1).

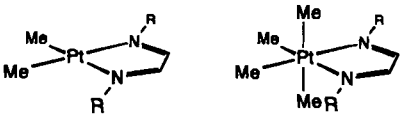

Fig. 1. R = C_6H_{11}.

Small platinum complexes have received increasing interest because of their medical importance, their model character for Pd-catalyzed transformations and reaction mechanisms in general, and their often conspicuous luminescence.[6] Owing to the presence of a 5d element with sizable spin-orbit coupling effects and possibly relativistic contributions to chemical bonding, a deeper understanding of coordination compounds of platinum requires a thorough experimental basis, preferably for small, theoretically accessible systems.

Results and Discussion

As a first surprise, both Pt^{II} and Pt^{IV} complexes in Figure 1 show almost identical responses in their cyclic voltammograms, that

[*] Prof. Dr. W. Kaim, Dipl.-Chem. S. Hasenzahl, Dr. H.-D. Hausen
Institut für Anorganische Chemie der Universität
Pfaffenwaldring 55, D-70550 Stuttgart (Germany)
Telefax: Int. code + (711)685-4241
e-mail: ak-kaim@rus.uni-stuttgart.de

  0570-0833/95/0101-0095 $ 10.00+.25/0

is, a reversible reduction at about -1.9 V vs. ferrocene/ferrocenium and an irreversible oxidation around $+0.4$ V (Fig. 2, Table 1). Furthermore, both complexes are intensely colored and highly solvatochromic (negative solvatochromism[7]); the absorption spectra show one band system in the visible and one

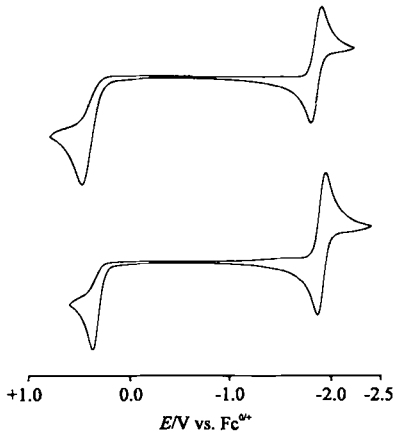

Fig. 2. Cyclic voltammograms of complexes [(CyN=CH–CH=NCy)PtMe$_n$] ($n = 2$: top, $n = 4$: bottom) in acetonitrile/0.1 M Bu_4NPF_6.

Table 1. Spectroscopic comparison of complexes [(CyN=CH–CH=NCy)PtMe$_n$].

		$n = 2$	$n = 4$
Cyclic voltammetry [a]:	E_{red}	-1.84	-1.93
	E_{ox} [b]	$+0.47$	$+0.37$
Absorption spectroscopy [c]:			
Neutral complexes [d]:	λ_{max1}	578 [e] (565,531)	532(505,485)
	λ_{max2}	400(382,376)	326(320,311)
Anionic complexes [f]:	λ_{max1}	540 [g]	354 [h]
	λ_{max2}	371	320
EPR of anionic complexes [i]:			
Fluid solution (295 K):	$\langle g \rangle$	2.016	1.9945
	a	n.o.	6.12(^{195}Pt)
			0.82(^{14}N)
			0.42(^{1}H, CH(DAB))
Frozen solution [j]:	g_1	2.090	2.003
	g_2	2.0163	2.003
	g_3	1.944 [k]	1.9776 [k]
	a_2(^{195}Pt)	6.5	7.5

[a] From measurements in CH_3CN/0.1 M Bu_4NPF_6, scan rate 100 mVs^{-1}. Potentials E in V vs. ferrocene/ferrocenium. [b] Anodic peak potentials for irreversible processes. [c] Absorption maxima λ_{max} in nm. [d] Values in toluene (THF, acetonitrile). [e] Shoulders at 650, 539, 498 nm. [f] From spectroelectrochemistry in THF/0.1 M Bu_4NPF_6. [g] Shoulders at 650, 508, 400 nm. [h] Shoulder at 415 nm. [i] From electrolyses in THF/0.1 M Bu_4NPF_6. Coupling constants a in mT. [j] At 4 K ($n = 2$) or at 110 K ($n = 4$). [k] Superhyperfine structure.

in the near-ultraviolet region (Fig. 3). The absorptions of the Pt^{II} species [Eq. (a)] occur at longer wavelengths. It exhibits a

$$[(CyN{=}CH{-}CH{=}NCy)Pt^{II}Me_2] \xrightarrow[MLCT]{h\nu} [(CyN{=}CH{-}CH{=}NCy)^{-1}Pt^{III}Me_2]^* \quad (a)$$

weak triplet transition at low energies (^{3}MLCT) and vibrational structuring of the first ^{1}MLCT band ($\Delta\nu \approx 1400$ cm^{-1}) due to the lower coordination number (diminished vibrational broadening).[8] The Pt^{IV} complex, on the other hand, exhibits a less intense but more solvatochromic absorption band in the visible region (Table 1).[9]

A truly important difference, however, is the very pronounced photoreactivity of [(CyN=CH–CH=NCy)PtMe$_4$] towards ambient light and on irradiation into the long-wavelength

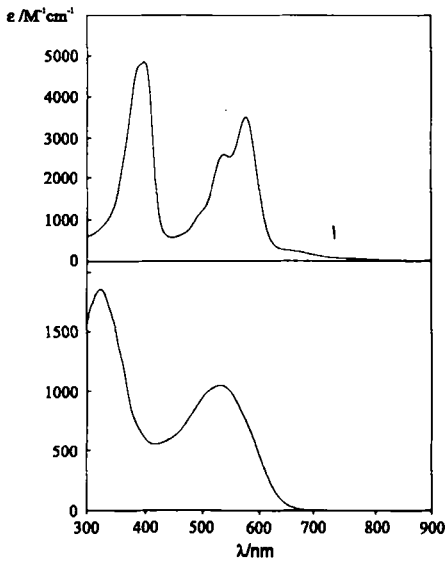

Fig. 3. Absorption spectra of complexes [(CyN=CH–CH=NCy)PtMe$_n$] ($n = 2$: top, $n = 4$: bottom) in toluene (absorbance different for each spectrum).

band ($\lambda > 500$ nm, cut-off filters). Not unexpectedly,[4] the result is a migration of methyl groups from the metal to the DAB ligand;[9] this implies that a photoinduced metal/alkyl bond homolysis is involved.[10, 11] A similar reaction and similar products were reported for the light-induced group transfer in [(RN=CH–CH=NR)ZnR'$_2$], where the single electron transfer from the asymmetric σ_{M-C} bond combination to the π^* MO of the DAB ligand was suggested as primary process.[4] By analogy to this interpretation and the results reported for heteroaromatic complexes of $PtMe_4$[10a] or $PtMe_3I$,[10b] we attribute the long-wavelength absorption of the Pt^{IV} complex to an LLCT transition originating from an asymmetric axial Pt–C σ bond combination (Fig. 4) to the π^* orbital of CyN=CH–CH=NCy [Eq. (b)]. In contrast, the

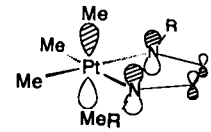

Fig. 4.

$$[(CyN{=}CH{-}CH{=}NCy)Pt^{IV}Me_4] \xrightarrow[LLCT]{h\nu} [(CyN{=}CH{-}CH{=}NCy)^{-1}Me_3Pt^{IV}{\cdot}Me]^* \xrightarrow{homolysis} \quad (b)$$

long-wavelength absorption of [(CyN=CH–CH=NCy)PtMe$_2$] can be attributed to a more "conventional" MLCT excitation [Eq. (a)], $d_{xz}(Pt) \rightarrow \pi^*(DAB)$, which has been similarly observed, albeit with lower resolution, for several organometallic and halide complexes of Pt^{II} with heteroaromatic ligands such as 2,2'-bipyridine.[6c, 8, 12, 13] We attributed this lack of resolution to the overlap of MLCT transitions to the two α-diimine π^* orbitals, $b_1(\psi)$ and $a_2(\chi)$.[8c] In the absence of potential substrates for oxidative addition,[14] the Pt^{II} complex shows no photoreactivity on irradiation into the long-wavelength band.

The assumption of a particular photochemical activation of the axial Pt–C(alkyl) bonds in the Pt^{IV} complex rests not only on theoretical considerations involving a σ_{M-C}/π^* interaction (Fig. 4)[4, 11] and on the observed photostability of the Me_2Pt^{II} system, but also on structural results obtained from a single-crystal diffraction study of [(CyN=CH–CH=NCy)PtMe$_4$] (Fig. 5). Crystal data and information on the data collection,

0570-0833/95/0101-0096 $ 10.00+.25/0 Chem. Eur. J. 1995, 1, No. 1

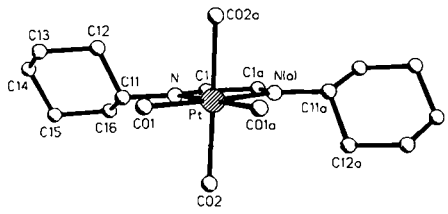

Fig. 5. Molecular structure of [(CyN=CH–CH=NCy)PtMe$_4$].

structure solution, and refinement are summarized in ref. [15] and in the Experimental Section. The results of the structure analysis are presented in Tables 2–4.

Table 2. Atomic coordinates ($\times 10^4$) and equivalent isotropic displacement parameters (pm^2) for [(CyN=CH–CH=N)PtMe$_4$]. U(eq) is defined as one third of the trace of the orthogonalized Uij tensor.

Atom	x	y	z	U(eq)
Pt	0	3206(1)	2500	178(1)
N	566(2)	1114(6)	3467(4)	243(13)
C(11)	1189(2)	1227(6)	4507(4)	237(14)
C(12)	955(3)	1717(6)	5502(5)	289(17)
C(13)	1606(4)	2074(7)	6585(6)	385(21)
C(14)	2106(3)	602(7)	6886(5)	368(18)
C(15)	2315(3)	47(8)	5879(5)	391(19)
C(16)	1660(3)	−309(7)	4814(4)	321(17)
C(1)	311(3)	−296(6)	3013(4)	289(16)
C(01)	573(3)	5071(6)	3525(5)	272(15)
C(02)	748(3)	3262(5)	1651(6)	298(19)

Table 3. Selected bond lengths (pm) for [(CyN=CH–CH=NCy)PtMe$_4$] [a].

Pt–N	215.0(4)	N–C11	145.5(5)
Pt–C01	204.5(5)	N–C1	129.2(7)
Pt–C02	214.0(8)	C1–C1(a)	144.0(9)

[a] Average C–C bond lengths (pm) for cyclohexyl: 153.1(8) (151.4–154.1).

Table 4. Bond angles (°) for [(CyN=CH–CH=NCy)PtMe$_4$] [a].

N-Pt-C01	98.9(2)	C02-Pt-C02(a)	177.6(2)
N-Pt-C02	88.2(2)	Pt-N-C11	124.8(3)
C01-Pt-C02	87.4(2)	Pt-N-C1	113.1(3)
N-Pt-N(a)	76.8(2)	C11-N-C1	122.1(4)
C01-Pt-N(a)	175.5(2)	N-C11-C12	108.9(4)
C02-Pt-N(a)	93.7(2)	N-C11-C16	115.9(4)
C01-Pt-C01(a)	85.5(3)	N-C1-C1(a)	118.5(3)
C02-Pt-C01(a)	90.8(2)		

[a] Average C-C-C bond angles (°) for cyclohexyl: 110.8(5) (109.5–112.3).

The molecular structure of [(CyN=CH–CH=NCy)PtMe$_4$] reveals the expected chelating mode of the DAB ligand with typical bond parameters for essentially nonreduced α-diimines.[16] The 5d^6-configurated metal center exhibits near-octahedral coordination, however, there is a clear distinction between Pt–Me bond lengths for the axial and equatorial substituents. As has been observed in similar cases,[17] the axial bonds are significantly longer than the equatorial ones; this illustrates a selective bond labilization even before the activation by light and the population of a dissociative LLCT excited state.

The difference in the arrangement of frontier orbitals in Pt^{II} and Pt^{IV} complexes, which is responsible for the very dissimilar photoreactivity, can be studied by means of the distinctly different absorption and EPR spectra (Fig. 6, Table 1) of the one-electron reduced forms of both d^6 and d^8 metal complexes [Eq. (c)].

$$[(CyN{=}CH{-}CH{=}NCy)Pt^{n}Me_n] \xrightarrow{e^-} [(CyN{=}CH{-}CH{=}NCy)^{-\cdot}Pt^{n}Me_n]^{-\cdot} \quad (c)$$

At room temperature, the chemically (with K) or electrolytically generated complex [(CyN=CH–CH=NCy)PtMe$_4$]$^{-\cdot}$ shows the characteristic EPR spectrum of a transition metal radical-anion complex,[18,19] that is, resolution of typical ligand hyperfine splitting[2,4] and moderate metal isotope coupling[18,19] (^{195}Pt: 33.7% natural abundance, $I = 1/2$, $A_{iso} = 370.9$ mT[20]) is observed. The g anisotropy measured in glassy frozen solution is

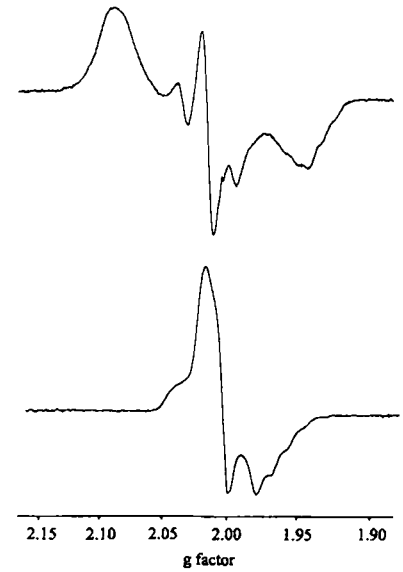

Fig. 6. EPR spectra in frozen solution of complexes [(CyN=CH–CH=NCy)-PtMe$_n$]$^{-\cdot}$ ($n = 2$: top, 4 K; $n = 4$: bottom, 110 K) as obtained from electrolysis in THF/0.1 M Bu_4NPF_6.

small, and the average g factor is lower than the free-electron value of 2.0023; this indicates an orbital arrangement with close-lying excited states of higher orbital angular momentum.[18] Such states and the resulting low g factors of anion radical complexes are often associated with high photoreactivity of the nonreduced forms of other d^6 systems involving Mn^{I},[21] Ru^{II},[22] or Mo^{0}.[23]

On the other hand, the one-electron reduced complex [(CyN=CH–CH=NCy)PtMe$_2$]$^{-\cdot}$ shows an unresolved EPR line at a relatively high isotropic g value of 2.016 and, in the frozen state, the g anisotropy $\Delta g = g_1 - g_3$ is 0.146, a much larger value than the $\Delta g = 0.0254$ of the Pt^{IV} complex (Table 1). Although these spectral data are still incompatible with a true Pt^{I} complex,[19] this result suggests a sizable metal contribution to the singly occupied MO. The large spin-orbit coupling constant of Pt^{II}[20] thus permits a clear distinction between the frontier orbital structures of both complexes discussed: the high g factor of the reduced Pt^{II} complex indicates a closeness of occupied d orbitals to the singly occupied π*(DAB) MO and a large energy gap to higher unoccupied orbitals, including σ_{Pt-C} MOs and the destabilized $d_{x^2-y^2}$ orbital. A comparison of schematic orbital diagrams for Pt^{II} and Pt^{IV} species illustrates the different electronic structures that are present despite the similar frontier orbital gaps (Fig. 7).

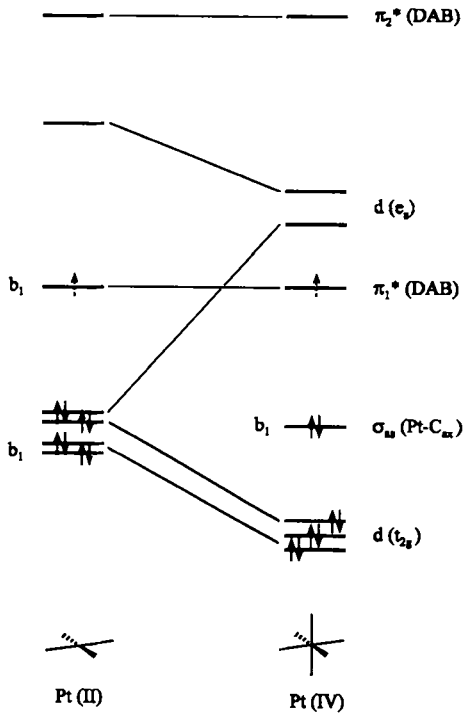

Fig. 7. Orbital diagrams for [(CyN=CH–CH=NCy)PtMe$_n$].

The different electronic structures of one electron reduced Pt^{II} and Pt^{IV} complexes are also reflected by dissimilar absorption spectra observed by UV/Vis spectroelectrochemistry (Table 1). Whereas $[(CyN{=}CH{-}CH{=}NCy)PtMe_4]^{-\cdot}$ shows a complete loss of the absorption features in the visible region, the platinum(II) species $[(CyN{=}CH{-}CH{=}NCy)PtMe_2]^{-\cdot}$ exhibits only a slight hypsochromic shift of the long-wavelength band. Detailed assignments of the observed transitions will have to await the results of calculations on these open-shell heavy-metal complexes.

Conclusion

We have shown that standard electrochemical and absorption spectroscopic studies can give very similar results for this particular type of Pt^{II} and Pt^{IV} organometallic complexes, in spite of rather different electronic structures. More sensitive techniques such as EPR of reduced species are able to point out these differences in greater detail and may thus help the interpretation of the significantly different chemical behavior.

Experimental Section

All experiments were carried out under an atmosphere of dry argon with freshly purified solvents. Starting materials CyN=CH–CH=NCy [3], $Pt_2Me_4(\mu\text{-}SMe_2)_2$ [24], and $Pt_2Me_8(\mu\text{-}SMe_2)_2$ [25] were prepared following literature procedures.

[(CyN=CH–CH=NCy)PtMe$_2$]: A solution of $[Pt_2Me_4(SMe_2)_2]$ (0.115 g, 0.2 mmol) and CyN=CH–CH=NCy (88 mg, 0.4 mmol) in benzene (15 mL) and diethyl ether (10 mL) was stirred overnight at ambient temperature. After removal of the solvent, the residue was dissolved in the minimum amount of Et_2O (about 7 mL), and the purple product crystallized in 40% yield (71 mg) at −30 °C. ^{1}H NMR (250 MHz, $CDCl_3$, 25 °C, TMS): δ = 1.00–1.73 (m, 10H; CH_2), 1.40 (t, 6H; CH3), 4.18 (m, 1H; CH(Cy)), 8.91 (t, 2H; CH(DAB)); $^2J(^{195}Pt{-}CH_3)$ = 84.9, $^3J(^{195}Pt{-}CH(DAB))$ = 35.0 Hz. ^{13}C NMR ($CDCl_3$): δ = −15.05 (CH_3), 25.59, 25.75, 33.79 (CH_2), 64.99 (CH(Cy)), 158.24 (CH(DAB)); $^1J(^{195}Pt{-}CH_3)$ = 785.5, $^2J(^{195}Pt{-}CH(Cy))$ = 36.4, $^2J(^{195}Pt{-}CH(DAB))$ = 14.5 Hz; $C_{16}H_{30}N_2Pt$ (445.5): calcd C 43.14, H 6.79, N 6.29%; found C 43.29, H 6.60, N 6.02%.

[(CyN=CH–CH=NCy)PtMe$_4$]: A solution of $[Pt_2Me_8(SMe_2)_2]$ (0.127 g, 0.2 mmol) in diethyl ether (20 mL) was treated under subdued light with CyN=CH–CH=NCy (88 mg, 0.4 mmol) for 16 h. Reduction of the volume to about 50% and subsequent cooling to −30 °C led to precipitation of a purple solid in 45% yield (86 mg). ^{1}H NMR (250 MHz, $CDCl_3$, 25 °C, TMS): δ = −0.54 (t, 6H; CH_3(ax)), 0.75 (t, 6H; CH_3(eq)), 1.13–2.06 (m, 10H; CH_2), 4.10 (m, 1H; CH(Cy)), 8.54 (t, 2H; CH(DAB)); $^2J(^{195}Pt{-}CH_3(ax))$ = 45.9, $^2J(^{195}Pt{-}CH_3(eq))$ = 71.3, $^3J(^{195}Pt{-}CH(DAB))$ = 31.6 Hz. ^{13}C NMR ($CDCl_3$): δ = −7.21 (CH_3(eq)), 2.69 (CH_3(ax)), 25.53, 25.64, 33.50 (CH_2), 65.11 (CH(Cy)), 155.37 (CH(DAB)); $^1J(^{195}Pt{-}CH_3(eq))$ = 694.0, $^1J(^{195}Pt{-}CH_3(ax))$ = 442.4, $^2J(^{195}Pt{-}CH(Cy))$ = 18.4 Hz; $C_{18}H_{36}N_2Pt$ (475.6): calcd C 45.46, H 7.63, N 5.89%; found C 45.86, H 7.46, N 5.83%. Crystals for X-ray diffraction were obtained from an acetone solution by slow cooling to −5 °C. For further details see ref. [15].

Instrumentation: EPR spectra were recorded in the X band on a Bruker System ESP300 equipped with a Bruker ER035M gaussmeter, a HP5350B microwave counter, and an Oxford cryostat ESR900. ^{1}H and ^{13}C NMR spectra were taken on a Bruker AC250 spectrometer. UV/Vis absorption spectra were recorded on Shimadzu UV160 and Bruins Instruments Omega 10 spectrophotometers. Cyclic voltammetry was carried out in acetonitrile/0.1 M Bu_4NPF_6 using a three-electrode configuration (glassy carbon electrode, Pt counter electrode Ag/AgCl reference) and a PAR273 potentiostat and function generator. The ferrocene/ferrocenium couple served as internal reference. Spectroelectrochemical measurements were performed using an optically transparent thin-layer electrode (OTTLE) cell [28] for UV/Vis spectra and a two-electrode capillary for EPR studies [22].

Acknowledgments: This work has been supported by the Landesforschungsschwerpunktprogramm Baden-Württemberg, the Volkswagenstiftung, and the Fonds der Chemischen Industrie. We thank Dr. Jan Fiedler (Prague) for assistance with the spectroelectrochemical measurements.

Received: October 24, 1994 [F6]

[1] a) G. van Koten, K. Vrieze, *Adv. Organomet. Chem.* **1981**, *21*, 151; b) G. van Koten, K. Vrieze, *Recl. Trav. Chim. Pays-Bas* **1981**, *100*, 129.
[2] H. tom Dieck, K.-D. Franz, F. Hohmann, *Chem. Ber.* **1975**, *108*, 163.
[3] H. tom Dieck, I. W. Renk, *Chem. Ber.* **1971**, *104*, 110 and **1972**, *105*, 1403.
[4] a) M. Kaupp, H. Stoll, H. Preuss, W. Kaim, T. Stahl, G. van Koten, E. Wissing, W. J. J. Smeets, A. L. Spek, *J. Am. Chem. Soc.* **1991**, *113*, 5606; b) E. Wissing, E. Rijnberg, P. A. van der Schaaf, K. van Gorp, J. Boersma, G. van Koten, *Organometallics* **1994**, *13*, 2609.
[5] a) R. W. Balk, D. J. Stufkens, A. Oskam, *Inorg. Chim. Acta* **1978**, *28*, 133; b) H. K. van Dijk, J. J. Kok, D. J. Stufkens, A. Oskam, *J. Organomet. Chem.* **1989**, *362*, 163; c) H. tom Dieck, L. Stamp, *Z. Naturforsch.* **1990**, *45b*, 1369.
[6] a) B. K. Keppler (Ed.), *Metal Complexes in Cancer Chemotherapy*, VCH, Weinheim, **1993**; b) G. van Koten, *Pure Appl. Chem.* **1989**, *61*, 1681; c) V. H. Houlding, V. M. Miskowski, *Coord. Chem. Rev.* **1991**, *111*, 145.
[7] a) C. Reichardt, *Solvents and Solvent Effects in Organic Chemistry*, 2nd ed., VCH, Weinheim, **1988**; b) D. M. Manuta, A. J. Lees, *Inorg. Chem.* **1983**, *22*, 3825; c) W. Kaim, S. Kohlmann, S. Ernst, B. Olbrich-Deussner, C. Bessenbacher, A. Schulz, *J. Organomet. Chem.* **1987**, *321*, 215.
[8] a) C. Vogler, B. Schwederski, A. Klein, W. Kaim, *J. Organomet. Chem.* **1992**, *436*, 367; b) A. Klein, H.-D. Hausen, W. Kaim, *J. Organomet. Chem.* **1992**, *440*, 207; c) W. Kaim, A. Klein, *Organometallics*, in press.
[9] Details of solvatochromism and photoreactivity as a function of the group R in complexes $[(RN{=}CH{-}CH{=}NR)PtMe_4]$ will be the subject of a forthcoming publication. Preparative photolysis studies of $[(RN{=}CH{-}CH{=}NR)PtMe_4]$ with R = 4-MeC_6H_4 yield product mixtures with both C- and N-methylation. The system with R = *t*Bu also yields some dehydrogenated C-alkylated product after hydrolysis, similar to that reported for the organozinc-based reaction in ref. [4b]. Photolysis is efficient, but does not proceed in a way that affects absorption spectroscopy within the usual scanning periods.
[10] a) J. E. Hux, R. J. Puddephatt, *J. Organomet. Chem.* **1988**, *346*, C31; b) H. Kunkely, A. Vogler, *Coord. Chem. Rev.* **1991**, *111*, 15.
[11] a) L. A. Lucia, R. D. Burton, K. S. Schanze, *Inorg. Chim. Acta* **1993**, *453*, 103.; b) H. Kunkely, A. Vogler, *J. Organomet. Chem.* **1993**, *453*, 269; c) S. Hasenzahl, W. Kaim, T. Stahl, *Inorg. Chim. Acta* **1994**, *225*, 23; d) C. Kutal, N. Serpone (Eds.), *Photosensitive Metal-Organic Systems*, ACS Adv. Chem. Ser. 238, Washington, **1992**.
[12] a) R. D. Kelly, G. B. Young, *J. Organomet. Chem.* **1989**, *361*, 123; b) N. Chaudhury, R. J. Puddephatt, *J. Organomet. Chem.* **1975**, *84*, 105.
[13] J. Biedermann, G. Gliemann, U. Klement, K.- J. Range, M. Zabel, *Inorg. Chem.* **1990**, *29*, 1884 and *Inorg. Chim. Acta* **1990**, *169*, 63.
[14] L. Chassot, A. von Zelewsky, *Helv. Chim. Acta* **1986**, *69*, 1855.
[15] Crystal data for $[(CyN{=}CH{-}CH{=}N)PtMe_4]$: Single-crystal preparation: crystallized from acetone, separated under Nujol; sealed in a capillary tube. $C_{18}H_{36}N_2Pt$, M_r = 475.6 g mol^{-1}, monoclinic, space group *C*2/*c*, *a* = 2021.6(2), *b* = 805.3(1), *c* = 1254.2(1) pm, β = 111.05(1)°, *V* = 1905.7(4) ×

10^6 pm^3, $Z = 4$, $\rho_{calcd} = 1.658$ g cm^{-3}, crystal size $0.4 \times 0.3 \times 0.12$ mm^3, deep-red thin plates, no. of reflections for lattice parameters = 36 ($18 \le 2\theta \le 23°$), $T = 173$ K, $\mu = 7.361$ mm^{-1}, $F(000) = 944$. Data collection and corrections: Siemens P4 diffractometer; $Mo_{K\alpha}$ radiation; graphite monochromator; variable scan speed ($3-60°$ min^{-1}); scan width = 1.1°; no. of standard reflections = 2 (every 98 measured); ω-scan collection method; $3 \le 2\theta \le 56°$; index ranges: $0 \le h \le 26$, $-10 \le k \le 0$, $-16 \le l \le 15$; 2351 reflections collected, 2284 of which independent, 2168 observed ($F > 4\sigma(F)$); corrections: Lorentz, polarization, absorption (semi-empirical ψ scan); min./max. transmission: 0.3712/0.9146; scattering factors: Int. Tables for X-Ray Crystallography [26]. Solution and refinement: structure solution by Patterson method; full-matrix least-squares refinement, 96 parameters refined; quantity minimized: $\Sigma w(F_o - F_c)^2$; anisotropic displacement coefficients for non-hydrogen atoms; hydrogen atoms in geom. pos. (C–H 96 pm), riding model, fixed U_{iso}; $R1 = \Sigma(|F_o| - |F_c|)/\Sigma|F_o| = 0.031$; $R2 = [\Sigma w(|F_o| - |F_c|)^2/\Sigma w|F_o|^2]^{1/2}$ ($w = 1/\sigma^2(F) + 0.002F^2$) = 0.034; Goof = $[\Sigma w(|F_o| - |F_c|)^2/(n-p)]^{1/2} = 0.87$; $\Delta\rho$(max./min.) = 1.37/−2.02 × 10^{-6} e pm^{-3}; SHELXTL PC program system. Further details of the crystal structure investigation are available on request from the Fachinformationszentrum Karlsruhe GmbH, D-76344 Eggenstein-Leopoldshafen (FRG), on quoting the depository number CSD-58665.

[16] a) J. Wunderle, J. Scholz, R. Fröhlich, *Z. Kristallogr.* **1993**, *208*, 277; b) see also K.-H. Thiele, V. Lorenz, G. Thiele, P. Zönnchen, J. Scholz, *Angew. Chem.* **1994**, *106*, 1461; *Angew. Chem. Int. Ed. Engl.* **1994**, *33*, 1372.

[17] K.-H. Thiele, H. Windisch, H. Schumann, G. Kociok-Köhn, *Z. Anorg. Allg. Chem.* **1994**, *620*, 523, and references therein.

[18] W. Kaim, *Coord. Chem. Rev.* **1987**, *76*, 187.

[19] a) P. S. Braterman, J.-I. Song, C. Vogler, W. Kaim, *Inorg. Chem.* **1992**, *31*, 222; b) P. S. Braterman, J.-I. Song, F. M. Wimmer, S. Wimmer, W. Kaim, A. Klein, R. D. Peacock, *Inorg. Chem.* **1992**, *31*, 5084.

[20] B. A. Goodman, J. B. Raynor, *Adv. Inorg. Chem. Radiochem.* **1970**, *13*, 135.

[21] R. Gross, W. Kaim, *Inorg. Chem.* **1986**, *25*, 498.

[22] W. Kaim, S. Ernst, V. Kasack, *J. Am. Chem. Soc.* **1990**, *112*, 173.

[23] S. Ernst, S. Kohlmann, W. Kaim, *J. Organomet. Chem.* **1988**, *354*, 177.

[24] J. D. Scott, R. J. Puddephatt, *Organometallics* **1983**, *2*, 1643.

[25] M. Lashanizadehgan, M. Rashidi, J. E. Hux, R. J. Puddephatt, S. S. M. Ling, *J. Organomet. Chem.* **1984**, *269*, 317.

[26] *International Tables for Crystallography*, The Kynoch Press, Birmingham (**1974**).

[27] Siemens Analytical X-Ray Instruments SHELXTL PC, Release 4.1, May 1990.

[28] M. Krejcik, M. Danek, F. Hartl, *J. Electroanal. Chem.* **1991**, *317*, 179.

  0570-0833/95/0101-0099 $ 10.00+.25/0